

Green function approach to superconductivity in nanowires

R. Saniz, B. Partoens, and F. M. Peeters

Departement Fysica, Universiteit Antwerpen, Groenenborgerlaan 171, B-2020 Antwerpen, Belgium

(Received 27 November 2011; revised manuscript received 23 March 2012; published 3 April 2012)

Superconductivity in nanowires made of weak coupling superconductor materials is investigated using a Green function approach. We show that these are multigap systems in which the ratio $\Delta(T)/k_B T_c$ is to a large extent similar to what is observed in some high- T_c two-gap systems, such as MgB_2 and some of the Fe-based superconductors. On the other hand, because of confinement, the superfluid density has a temperature behavior of the form $n_s(T) = 1 - (T/T_c)^3$ near T_c , thus deviating from the BCS behavior for bulk superconductors.

DOI: [10.1103/PhysRevB.85.144504](https://doi.org/10.1103/PhysRevB.85.144504)

PACS number(s): 74.20.-z, 74.78.-w, 74.81.-g

I. INTRODUCTION

Interest in the effects of quantum confinement on superconductivity developed long before the advent of nanoscience.^{1–4} Advances in materials synthesis and nanolithography technology, however, makes it now possible to fabricate in a reproducible way high quality nanoscale samples, in which confinement effects can be examined in more detail. Nanowires have attracted particular interest in the past several years, leading to experimental studies in systems fabricated with a range of materials and methods. See Refs. 5–12 for a few examples. Among the most intriguing findings, we mention that in Al nanowires the superconducting critical temperature T_c was found to increase with decreasing radius of the nanowire, reaching values more than 50% higher than in the bulk.^{10,13} In the case of Sn nanowires, T_c appears to be less sensitive to the radius, but its value was reported to be higher than in the bulk in at least one sample.⁷ In the case of Pb nanowires, an enhancement of T_c was also observed in crystalline samples, but not in polycrystalline ones.⁵ In NbSe_2 nanowires, the critical field H_c was found to be 2–6 times larger than in the bulk, depending on the orientation of the field.⁸ Interestingly, an enhancement of H_c over its bulk value was already reported in a study of Sn “whiskers” in 1957.^{1,14}

On the theory side, work has been somewhat more sparse. See Ref. 15 for a recent review. For inhomogeneous superconductors, a powerful approach is given by the self-consistent field method of Bogoliubov and de Gennes (BdG).¹⁶ As discussed in previous works using this method, because of the quality of the nanowires in experiment, the effects of disorder are sufficiently low that the theoretical studies can be done in the clean limit.^{13,15,17} These works have led to several findings, greatly advancing our understanding of the effects of confinement on superconductivity. For instance, the spatial variation of the order parameter due to confinement was found to be much stronger than predicted by Ginzburg-Landau theory, and gapless superconductivity was predicted above a certain applied field.¹⁷ A most interesting finding is that the so-called shape resonances as a function of confining length, first discussed by Blatt and Thompson in 1963 in their study of superconductivity in thin films,^{2,3} also occur in nanowires.¹⁸ In fact, the enhancement of T_c depending on nanowire radius observed in experiment has been interpreted as due to these shape resonances.¹³ The effect of the latter in nanowires is found to be more dramatic than in nanofilms. Indeed, the

predicted enhancement of T_c or of the superconducting gap over their bulk values can be astounding.^{15,18} The reported effect on the coherence length is equally remarkable. Near resonance lengths of just a few nanometers are obtained, values more typical of strongly correlated superconductors such as the cuprates.¹⁹

In this work we use the Green functions formulation of the Bardeen, Cooper, and Schrieffer (BCS) theory of superconductivity,²⁰ first introduced by Gor’kov for homogeneous, bulk systems.²¹ The approach we follow has not been applied to nanowires previously, and we show here that it is indeed a very good alternative to the BdG method. It has the additional advantage that it lends itself to analytical work, so that most of the results can be written in closed form. This allows us to shed new light on the properties of superconductivity in nanowires with comparative ease. As in previous work,^{13,15,17} our study is done in the clean limit. Superconductivity in nanowires is quite extraordinary. First, because of confinement, superconductivity becomes multigap, although the bulk material may be a simple, single-gap superconductor such as Al. Then, as we show here, the $\Delta(T)/k_B T_c$ ratios, at $T = 0$ K as well as for $T \rightarrow T_c$, deviate from conventional BCS theory in a way that parallels what occurs in some conventional and unconventional two-gap systems with a high T_c , such as MgB_2 and LiFeAs . As one may expect, their position in a Inosov plot²² classifies them as weak coupling superconductors, even for T_c values that rival those of the cuprate superconductors. On the other, the superfluid density in these systems is a very small fraction of the total electron density, even at $T = 0$. Furthermore, due to confinement, for temperatures close to T_c its behavior as a function of temperature is different from the BCS behavior for bulk superconductors. Indeed, it shows a behavior that is nearly cubic in T/T_c , falling between the BCS local and nonlocal results.²⁰

In Sec. II we derive the mean-field solution to an effective superconducting Hamiltonian, with no particular assumption regarding the geometry of the system and only assuming an orthonormal independent quasiparticle basis. The purpose is to have a formulation general enough, but also explicit enough, that it can be readily applied to confined superconductors of almost any geometry, such as nanofilms, nanocylinders, nanoshells, etc. In Sec. III we present our results for nanowires. Section IV concludes with a discussion.

II. FORMALISM

We consider a system of quasiparticles in which an effective interaction v_{eff} couples those of opposite spin only. This is the net effect of phonon exchange and of the screened Coulomb interaction (for which an explicit form is not required at this point). The Hamiltonian of the system is

$$\hat{H} = \sum_{\sigma} \int d^3r \hat{\psi}_{\sigma}^{\dagger}(\mathbf{r}) [H_0(\mathbf{r}) - \mu] \hat{\psi}_{\sigma}(\mathbf{r}) + \frac{1}{2} \int d^3r d^3r' \hat{\psi}_{\uparrow}^{\dagger}(\mathbf{r}) \hat{\psi}_{\downarrow}^{\dagger}(\mathbf{r}') v_{\text{eff}}(\mathbf{r}, \mathbf{r}') \hat{\psi}_{\downarrow}(\mathbf{r}') \hat{\psi}_{\uparrow}(\mathbf{r}), \quad (1)$$

where H_0 is the Hamiltonian of the uncoupled quasiparticles and μ is the chemical potential. We seek to determine the system's single-particle temperature Green function, defined by $\mathcal{G}(\mathbf{r}\mathbf{r}', \tau) = -\langle T_{\tau} \hat{\psi}_{\uparrow}^{\dagger}(\mathbf{r}\tau) \hat{\psi}_{\uparrow}(\mathbf{r}'0) \rangle$ (we take here spin- \uparrow for definiteness). To solve the equation of motion for \mathcal{G} we introduce the Gorkov functions $\mathcal{F}(\mathbf{r}\mathbf{r}', \tau) = -\langle T_{\tau} \hat{\psi}_{\uparrow}^{\dagger}(\mathbf{r}\tau) \hat{\psi}_{\downarrow}(\mathbf{r}'0) \rangle$ and $\mathcal{F}^{\dagger}(\mathbf{r}\mathbf{r}', \tau) = -\langle T_{\tau} \hat{\psi}_{\downarrow}^{\dagger}(\mathbf{r}\tau) \hat{\psi}_{\uparrow}(\mathbf{r}'0) \rangle$, and take the mean-field approximation²⁰

$$\langle T_{\tau} \hat{\psi}_{\downarrow}^{\dagger}(\mathbf{r}_1\tau_1) \hat{\psi}_{\downarrow}(\mathbf{r}_2\tau_2) \hat{\psi}_{\uparrow}^{\dagger}(\mathbf{r}_3\tau_3) \hat{\psi}_{\uparrow}^{\dagger}(\mathbf{r}_4\tau_4) \rangle \simeq -\mathcal{F}(\mathbf{r}_3\mathbf{r}_2, \tau_3 - \tau_2) \mathcal{F}^{\dagger}(\mathbf{r}_1\mathbf{r}_4, \tau_1 - \tau_4). \quad (2)$$

The resulting coupled equations for \mathcal{G} and \mathcal{F}^{\dagger} read, in frequency domain,

$$\mathcal{L}_p(\mathbf{r}) \tilde{\mathcal{G}}(\mathbf{r}\mathbf{r}', \omega_p) - \int d^3r'' \Delta(\mathbf{r}\mathbf{r}'') \tilde{\mathcal{F}}^{\dagger}(\mathbf{r}''\mathbf{r}', \omega_p) = \hbar \delta(\mathbf{r} - \mathbf{r}'),$$

$$\mathcal{L}_p(\mathbf{r}) \tilde{\mathcal{F}}^{\dagger}(\mathbf{r}\mathbf{r}', \omega_p) - \int d^3r'' \Delta(\mathbf{r}\mathbf{r}'') \tilde{\mathcal{G}}(\mathbf{r}''\mathbf{r}', \omega_p) = 0. \quad (3)$$

Here $\mathcal{L}_p(\mathbf{r}) = i\hbar\omega_p - H_0(\mathbf{r}) + \mu$, with ω_p a fermionic frequency, denoting a τ -Fourier transformed function, and we have introduced $\Delta(\mathbf{r}\mathbf{r}'') \equiv v_{\text{eff}}(\mathbf{r}, \mathbf{r}'') \mathcal{F}(\mathbf{r}\mathbf{r}'', 0)$, that is, a nonlocal pairing potential,²³ also called pairing field in nuclear physics.²⁴ As we will see further down, it is the pairing potential that gives rise to the superconducting energy gap.

Let us now assume that the external potential in H_0 is spin independent and that the boundary conditions are such that the eigenstates of H_0 form an orthonormal set, that is, the quasiparticle states are given by $H_0|v\rangle = E_v|v\rangle$, with $\langle v|v'\rangle = \delta_{vv'}$. Hence, the field operators have the expansions $\hat{\psi}_{\sigma}(\mathbf{r}\tau) = \sum_v \psi_v(\mathbf{r}) c_{v\sigma}(\tau)$ and $\hat{\psi}_{\sigma}^{\dagger}(\mathbf{r}\tau) = \sum_v \psi_v^*(\mathbf{r}) c_{v\sigma}^{\dagger}(\tau)$. Projecting Eqs. (3) onto this basis, so that, for example, $\tilde{\mathcal{G}}(\mathbf{r}\mathbf{r}', \omega_p) = \sum_{vv'} \psi_v(\mathbf{r}) \psi_{v'}^*(\mathbf{r}') \tilde{\mathcal{G}}(vv', \omega_p)$, and $\tilde{\mathcal{F}}^{\dagger}(\mathbf{r}\mathbf{r}', \omega_p) = \sum_{vv'} \psi_v^*(\mathbf{r}) \psi_{v'}^*(\mathbf{r}') \tilde{\mathcal{F}}^{\dagger}(vv', \omega_p)$, yields

$$[i\hbar\omega_p - \epsilon_v] \tilde{\mathcal{G}}(vv', \omega_p) + \sum_{\mu} \Delta(v\mu) \tilde{\mathcal{F}}^{\dagger}(\mu v', \omega_p) = \hbar \delta_{vv'},$$

$$[i\hbar\omega_p + \epsilon_v] \tilde{\mathcal{F}}^{\dagger}(vv', \omega_p) + \sum_{\mu} \Delta^*(v\mu) \tilde{\mathcal{G}}(\mu v', \omega_p) = 0. \quad (4)$$

In the above we refer the energies with respect to the chemical potential and introduced $\epsilon_v = E_v - \mu$ and the gap matrix $\Delta(vv') = \sum_{\mu\mu'} V_{vv', \mu\mu'} \mathcal{F}(\mu\mu', 0)$, where $V_{vv', \mu\mu'} \equiv -\langle vv'|v_{\text{eff}}|\mu\mu'\rangle$.²⁵ We have then a block-matrix equation

$$\begin{pmatrix} \mathcal{E} & \mathcal{D} \\ \mathcal{D}^* & -\mathcal{E}^* \end{pmatrix} \begin{pmatrix} \tilde{\mathcal{G}} \\ \tilde{\mathcal{F}}^{\dagger} \end{pmatrix} = \begin{pmatrix} \mathcal{I} \\ \mathcal{O} \end{pmatrix}. \quad (5)$$

Here matrix \mathcal{D} is defined by $\mathcal{D}(vv') = \Delta(vv')/\hbar$ and $\mathcal{E}(vv') = \delta_{vv'}(i\omega_p - \epsilon_v/\hbar)$, while \mathcal{I} and \mathcal{O} are the identity and zero matrices, respectively. Thus, quite generally, $\tilde{\mathcal{G}}$ and $\tilde{\mathcal{F}}^{\dagger}$ are given in closed form by

$$\tilde{\mathcal{G}} = [\mathcal{E} + \mathcal{D}(\mathcal{E}^*)^{-1} \mathcal{D}^*]^{-1},$$

$$\tilde{\mathcal{F}}^{\dagger} = (\mathcal{E}^*)^{-1} \mathcal{D}^* [\mathcal{E} + \mathcal{D}(\mathcal{E}^*)^{-1} \mathcal{D}^*]^{-1}. \quad (6)$$

Note that up to now few assumptions were made as to the form or sign of the effective interaction, or of the geometry of the system. The task from here on is to determine the gap matrix that satisfies the above implicit system.

We now assume that the effective interaction couples only time-reversed states,²⁶ and that it is attractive. For notational simplicity, in the following the time-reversed state corresponding to ψ_v is written ψ_{-v} . The effective interaction matrix elements introduced above become

$$V_{vv', \mu\mu'} = V_{v-v, \mu-\mu} \delta_{-v v'} \delta_{-\mu \mu'} \equiv V_{v\mu} \delta_{-v v'} \delta_{-\mu \mu'}, \quad (7)$$

and the gap matrix becomes $\Delta(vv') = \delta_{-vv'} \sum_{\mu} V_{v\mu} \mathcal{F}(-\mu \mu, 0) \equiv \Delta(v) \delta_{-vv'}$. It is straightforward to deduce from Eqs. (6) that the Green and Gorkov functions are then given by

$$\tilde{\mathcal{G}}(vv', \omega_p) = -\delta_{vv'} \frac{i\omega_p + \epsilon_v/\hbar}{\omega_p^2 + \xi_v^2/\hbar^2},$$

$$\tilde{\mathcal{F}}^{\dagger}(vv', \omega_p) = \delta_{-vv'} \frac{\Delta^*(v)/\hbar}{\omega_p^2 + \xi_v^2/\hbar^2}, \quad (8)$$

with $\xi_v^2 = \epsilon_v^2 + |\Delta(v)|^2$. Thus, the coefficients of the expansion of the pairing potential over the quasiparticle basis are indeed the superconducting energy gap values. Noting that $\mathcal{F}(-\mu \mu, 0) = \sum_p \tilde{\mathcal{F}}(-\mu \mu, \omega_p)/\beta\hbar$, and with the above solution for the Gorkov function, the expression for $\Delta(v)$ finally becomes

$$\Delta(v) = \sum_{v'} V_{vv'} \Delta(v') \frac{1}{2\xi_{v'}} \tanh \frac{\xi_{v'}}{2k_B T}. \quad (9)$$

This equation determines both the gap values and the critical temperature [so, in fact $\Delta(v) = \Delta(v, T)$]. Once the $\Delta(v)$ are determined, other quantities can be calculated. Furthermore, one can calculate the order parameter, or condensate wave function, which can be defined by $\Psi(\mathbf{r}\mathbf{r}') \equiv \mathcal{F}(\mathbf{r}\mathbf{r}', 0)$.²⁷ It can be readily shown that one has

$$\Psi(\mathbf{r}\mathbf{r}') = \sum_v \psi_v(\mathbf{r}) \psi_{-v}(\mathbf{r}') \Delta(v) \frac{1}{2\xi_v} \tanh \frac{\xi_v}{2k_B T}. \quad (10)$$

The pairing potential, a quantity of interest in its own right,²⁴ can be calculated through the back-projection

$$\Delta(\mathbf{r}\mathbf{r}') = \sum_v \psi_v(\mathbf{r}) \psi_{-v}(\mathbf{r}') \Delta(v). \quad (11)$$

Let us point out here the following. If one assumes that the effective interaction is given by a δ function²⁰ $v_{\text{eff}}(\mathbf{r} - \mathbf{r}') = -V_0 \delta(\mathbf{r} - \mathbf{r}')$, then the pairing potential is equally ill-defined [cf. the definition above, after Eq. (3)] because the Dirac δ function is not a proper function. Nonetheless, since Eqs. (3) are integral equations, a δ function interaction still leads to a well defined pair of coupled equations. From these, the gap

equation is derived by introducing the so-called gap function $\Delta(\mathbf{r}) = V_0 \mathcal{F}(\mathbf{r}, 0)$.²⁰ Therefore, in such an approach, the order parameter and the gap function differ only by a multiplicative constant and can be treated as essentially the same quantity. However, the gap function concept loses its usefulness when studying inhomogeneous systems, and a more natural role is played by the pairing potential. It is important to keep in mind that the latter is not equivalent to the order parameter.

III. MULTIGAP SUPERCONDUCTIVITY IN NANOWIRES

For definiteness, in the following we take parameters corresponding to Al,²⁸ which is a weak coupling superconductor (so a mean-field approach is applicable), and is also free-electron-like. To model a nanowire we consider a system of quasiparticles in a cylindrical potential well of radius R and length L : $V(\rho, \phi, z) = 0$ for $\rho \leq R$, and ∞ otherwise ($R \ll L$). The quasiparticle states are¹⁷ $\psi_{kmn}(\rho, \phi, z) = [\pi R^2 L J_{|m|+1}^2(\eta_{mn})]^{-1/2} J_{|m|}(\rho \eta_{mn}/R) e^{i(kz+m\phi)}$, where J_m is the m th order Bessel function of the first kind and η_{mn} is its n th zero,³⁰ and $k = 2\pi l/L$, with $l \in \mathbb{Z}$. k is the momentum along the wire (we assume periodic boundary conditions along the z direction and take the limit $L \rightarrow \infty$ at the end of the calculation). The eigenenergies are given by $E_{kmn} = \hbar^2(k^2 + \eta_{mn}^2/R^2)/2m$, that is, a set of nonintersecting parabolae. For simplicity we assume that the quasiparticle effective mass is isotropic and equal to the bare electron mass. For given R , μ (the Fermi level) is determined by the particle density. The Fermi surface reduces to the discrete set of points $\{-k_F^{(mn)}, k_F^{(mn)}\}_{mn}$, where $k_F^{(mn)} = (2m\mu/\hbar^2 - \eta_{mn}^2/R^2)^{1/2}$ (the indices mn run over occupied bands only). Naturally the lower the band minimum (the lower the value of η_{mn}), the larger the Fermi momentum. Also, given a state $|\nu\rangle = |kmn\rangle$, its corresponding time-reversed state is $|\bar{\nu}\rangle = |-k -m n\rangle$. To solve the gap equation (9) we adopt a phenomenological approximation to the interaction matrix elements $V_{\nu\nu'}$. Following the standard BCS model for bulk superconductivity, we define²⁰

$$V_{kmn, k'm'n'} \equiv \frac{U_{mn, m'n'}}{\pi^2 R L} \theta(\epsilon_w - |\epsilon_{kmn}|) \theta(\epsilon_w - |\epsilon_{k'm'n'}|). \quad (12)$$

Thus the interaction is effective only within an energy window ϵ_w around μ . The magnitude of the coupling parameters $U_{mn, m'n'}$ is estimated with the help of a contact potential of strength V_0 , that is, $v(\mathbf{r} - \mathbf{r}') = -V_0 \delta(\mathbf{r} - \mathbf{r}')$. The above implicitly determines the effective interaction v_{eff} .³¹ The gap equation finally becomes

$$\Delta(mn) = \sum_{m'n'} U_{mn, m'n'} \Delta(m'n') \times \int_{-\epsilon_w}^{+\epsilon_w} d\epsilon \mathcal{N}_{m'n'}(\epsilon) \frac{1}{2\xi_{m'n'}} \tanh \frac{\xi_{m'n'}}{2k_B T}, \quad (13)$$

where we switched from the summation over k to an integral over energy introducing the density of states

$$\mathcal{N}_{mn}(\epsilon) = \frac{\theta(\epsilon - \hbar^2 \eta_{mn}^2 / 2m R^2 + \mu)}{2\pi \sqrt{\epsilon - \hbar^2 \eta_{mn}^2 / 2m R^2 + \mu}} \frac{1}{\pi R^2}, \quad (14)$$

with θ the Heaviside step function.³²

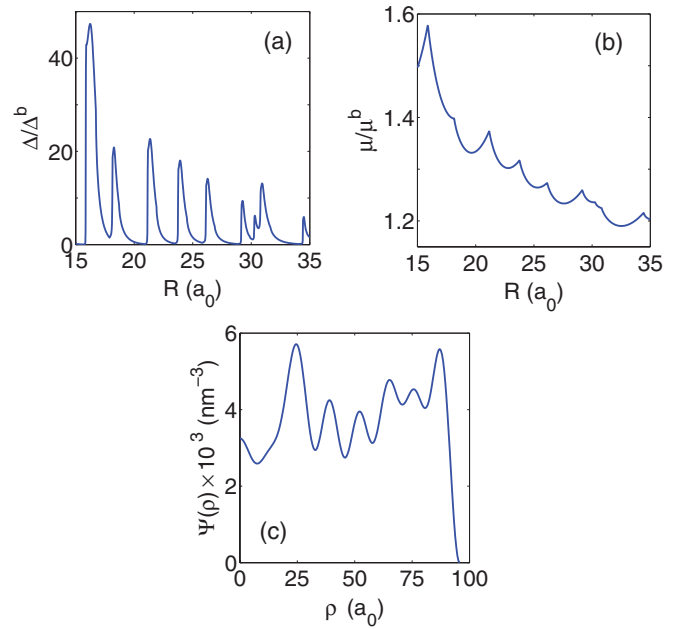


FIG. 1. (Color online) Gap, normalized to the bulk value [(a)] and chemical potential, also normalized to the bulk value [(b)] as a function of nanowire radius for a quasiparticle density of 3.878 nm^{-3} . (c) Order parameter as a function of center of mass coordinate ρ for a nanowire with radius 5.06 nm ($\sim 95.62 a_0$). The above is for the case in which all couplings have the same value in the gap equation.

Solving Eq. (13) results in multiple gaps, with a different gap value for each occupied band. But prior to further discussing our results here, we consider a system studied in Ref. 18 to show that the present approach describes essentially the same physics as the BdG method. Thus we take an electron density of 3.878 nm^{-3} and a bulk chemical potential of 900 meV (V_0 is denoted g in Ref. 18). We then consider the case in which the coupling parameters in the gap equation have all the same single value. Here we take their average value $U = \langle U_{mn, m'n'} \rangle$. This results in a single gap superconductor. In Figs. 1(a) and 1(b) we plot, respectively, the gap value (normalized to the bulk gap) and the chemical potential as a function of nanowire radius. In Fig. 1(c) we plot the order parameter at the center-of-mass coordinate $\Psi(\mathbf{r}, \mathbf{r})$, in which case Ψ depends only on the radial coordinate ρ and is invariant along the z direction. At $T = 0 \text{ K}$, from Eq. (10) it is straightforward to find

$$\Psi(\rho) = \frac{\Delta}{2\pi^2 R^2} \sum_{m \geq 0, n} I_{mn} (2 - \delta_{m0}) \frac{J_m^2(\rho \eta_{mn}/R)}{J_{m+1}^2(\eta_{mn})}, \quad (15)$$

with

$$I_{mn} = \int_{-\epsilon_w}^{+\epsilon_w} d\epsilon / 2 \sqrt{(\epsilon^2 + \Delta^2)(\epsilon - \hbar^2 \eta_{mn}^2 / 2m R^2 + \mu)}. \quad (16)$$

The order parameter is plotted for a nanowire of radius 5.06 nm . The agreement between our results and those in Figs. 1 and 2 of Ref. 18 is indeed remarkable. As a matter of fact, seeking the solution of an effective superconducting Hamiltonian for an inhomogeneous system in terms of the set of uncoupled quasiparticles states was first proposed by Anderson for dirty superconductors.²⁶ It appears that

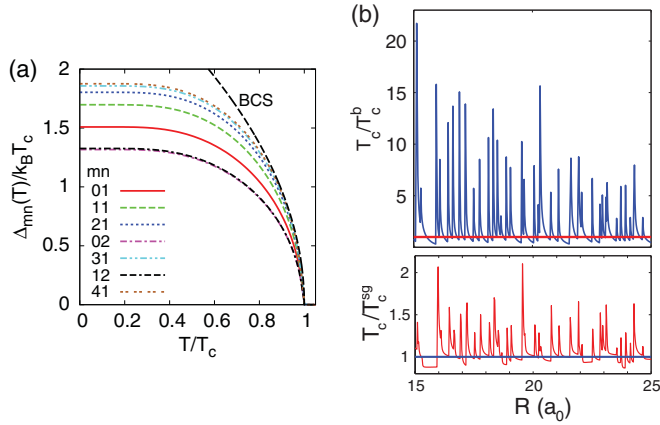


FIG. 2. (Color online) (a) Plot of the seven $\Delta_{mn}(T)$ in a $R = 7.5 a_0$ nanowire; $T_c = 4.2T_c^b$. For comparison, the dashed line indicates the BCS expression $\Delta(T)/k_B T_c = 3.06(1 - T/T_c)^{1/2}$. (b) *Upper panel*: T_c as a function of R . T_c increases sharply when a new band starts to be occupied. The horizontal line indicates T_c^b . For large R , T_c tends to T_c^b (not shown here). *Lower panel*: The ratio of T_c to the single-gap value T_c^{sg} shows that they differ significantly.

subsequently the scheme fell in disfavor compared to the BdG method. However, more recently, Tanaka and Marsiglio³³ used the attractive Hubbard model to compare the Anderson scheme and the BdG method. Studying surfaces and impurities, they found that in the weak coupling regime the Anderson scheme captures in fact the essential features of the BdG method.³³ Our results above are thus in line with the findings of Tanaka and Marsiglio.

As already indicated, in the more general case further up, the gap equation will result in multiple gaps, with a different gap value for each occupied band. The number of occupied bands increases rapidly with radius. For illustrative purposes, we consider a nanowire with only a few bands occupied, that is, small radius. In Fig. 2(a) we plot the gap values as a function of temperature for a nanowire of radius $R = 7.5 a_0$ (a_0 denoting the Bohr radius). In this case there are seven occupied bands, hence seven energy gap values. The critical temperature is $4.2T_c^b$, that is, at this radius there is a fourfold enhancement with respect to the bulk value. The dependence on radius is discussed further down. The ratios $\Delta_{mn}(0)/k_B T_c$ vary between 1.32 and 1.88. Thus, some of the ratios are below the BCS value (1.76),²⁰ and some are above. This is akin to what occurs in many of the known two-gap superconductors, including Fe-based superconductors such as LiFeAs, in which the smaller gap has a ratio below the BCS value, while the larger gap has a ratio above that value.²² The behavior of the gap value with temperature is also interesting. The long-dash line in Fig. 2(a) indicates the conventional BCS result $\Delta(T)/k_B T_c = 3.06(1 - T/T_c)^{1/2}$ for $T_c - T \ll T_c$.²⁰ Assuming that the square root behavior near T_c also holds in the present case, we find that the universal proportionality constant 3.06 has to be replaced by constants in the interval (2.04, 3.06), with different values for the different gaps. Hence, approaching T_c the gaps tend to close faster than in conventional BCS theory. Also, our results indicate that the ratio of the different gaps near T_c deviate slightly from a constant value, with the smaller gaps tending more rapidly to zero at T_c . This means that there is

a deviation from the square root behavior near T_c . The above shows similarities with MgB₂. Indeed, the theoretical study in Ref. 34 finds that both gaps in MgB₂ have a square root behavior for $T \rightarrow T_c$, but that, as a consequence of interband coupling, the proportionality constants differ from the BCS value. Furthermore, in experiment it has been found that the ratio of the large gap to the small gap in MgB₂ increases with temperature near T_c , with the smaller gap tending more rapidly to zero than the larger gap.³⁵

The dramatic effects of confinement are best shown by the radius dependence of the critical parameters. The gap equation depends on radius essentially through the $U_{mn,m'n'}$ strengths and the density of states $\mathcal{N}_{nm}(\epsilon)$ [cf. Eq. (13)]. We consider the latter first. As R increases, the distance between the minima of the bands decreases and, at a certain point, a new band will be occupied. Whenever this happens the density of states has a drastic change, causing a sharp increase in the critical values, such as the energy gap. This is similar to what was found in nanofilms.^{2,3} As discussed in previous work, however,¹⁸ in nanowires the increase is particularly strong because the density of states has a van Hove singularity at the bottom of each band [cf. Eq. (14)]. As a consequence, the oscillations of the critical parameters as a function of R are very sharp and large. This is shown for T_c in Fig. 2(b), upper panel. The oscillations are stronger for smaller R , and slowly decrease with increasing R , as T_c tends to its bulk value. We call attention to the fact that because in nanowires the density of states is a rapidly varying function of energy, one cannot resort to a calculation of the critical parameters by making the approximation $\mathcal{N}_{nm}(\epsilon) \simeq \mathcal{N}_{nm}(0)$ within the energy window determined by ϵ_w . This is a long used approximation,^{16,20} and has also been used in the study of some of the recent multigap superconductors.³⁶ In essence, the density of states at the Fermi level renormalizes the coupling strength. But this is not a valid approximation here. We verified that applying such an approximation would lead to a severe underestimation of T_c and of the gap values (more than an order of magnitude for $R = 7.5 a_0$), even when no van Hove singularity is close to the Fermi level.

Before discussing the role of the coupling parameters $U_{mn,m'n'}$ we point out that their value can be affected by the electronic density of states, because the latter can affect the electron-phonon coupling strength.³⁷ This important aspect falls beyond the scope of the present study and is discussed further in Sec. IV. The role of the coupling parameters in Eq. (13) is twofold. First, they determine the degree of degeneracy of the gap values. This has an important quantitative and qualitative impact. For instance, if the couplings had all the same value, there would be a single gap, with further significant effect on the values of the critical parameters. To show this we replaced the $U_{mn,m'n'}$ by a single coupling strength, namely their average $\bar{U}_{mn,m'n'}$, and calculated the corresponding critical temperature, which we denote T_c^{sg} . In the lower panel of Fig. 2(b) we plot the ratio of T_c^{sg} and the T_c values in the upper panel. The difference between the two is manifest, with T_c values more than 100% higher than T_c^{sg} . At higher radii (not shown), as T_c tends gradually to its bulk value, the difference with the single-gap result vanishes.

Second, the $U_{mn,m'n'}$ determine to a large extent the relative weight of interband and intraband couplings and, therefore,

the relative magnitude of the energy gap values. In Fig. 2(a) the order of the band gap labels reflect how deep below the Fermi level (μ) are the minima of the different occupied bands; $mn = 01$ corresponds to the lowest band minimum and $mn = 41$ to the highest. One can see that a higher band minimum (van Hove singularity closer to the Fermi level) does not necessarily imply a larger gap. Indeed, the band minima for $mn = 01, 11$, and 21 , for instance, are well below the one for $mn = 12$, but the gap corresponding to the latter is smaller. Hence, not only the number of paired states counts, but also the quality of their coupling.

Given the high T_c values that can be reached at small radii [up to 26 K in the range of radii in Fig. 2(b)], it is of interest to make some comparison with the known high- T_c superconductors. Inosov and co-workers have recently made an extensive comparison of the ratio $2\Delta(0)/k_B T_c$ vs T_c for different families of superconductors, including conventional and unconventional superconductors.²² To calculate this ratio we have chosen an interval of radii such that T_c sweeps a large range of values. For R in the interval from 7 to $8 a_0$, T_c ranges from 0.29 K at $R = 8 a_0$ to 115 K at $R = 7.3 a_0$. The former and latter points are labeled A and B, respectively, in Fig. 3(a). Label C corresponds to the pair $R = 7.27 a_0$ and $T_c = 94$ K (below this radius the number of occupied bands drops from 7 to 6, and T_c decreases sharply to values close to those of point A). We calculate $2\Delta_{mn}(T)/k_B T_c$ for the range of radii comprised by points A, B, and C. For example, consider the curve for $mn = 01$ in Fig. 3(b). We see that the corresponding ratio has a value of 3.27 at the T_c corresponding to point A in Fig. 3(a), decreases to 2.57 at the T_c corresponding to B, and slightly increases to 2.67 at the T_c value of C.³⁸ The other gaps show similar but not equivalent behavior. As the figure shows, for the smaller gap values the ratio clearly falls below the weak coupling limit (3.52) in the Inosov plot, while it is slightly above for the larger gaps. The ratios found are close to those observed in other conventional multigap superconductors, such as MgB_2 , Mo_5Sb_7 , or $\text{YNi}_2\text{B}_2\text{C}$, but also some of the ferropnictide superconductors, such as those of the 111 family.²² Nonetheless, the ratios in the nanowires does not increase as T_c increases, in contrast to what occurs for most of the Fe-based and cuprate superconductors. This is

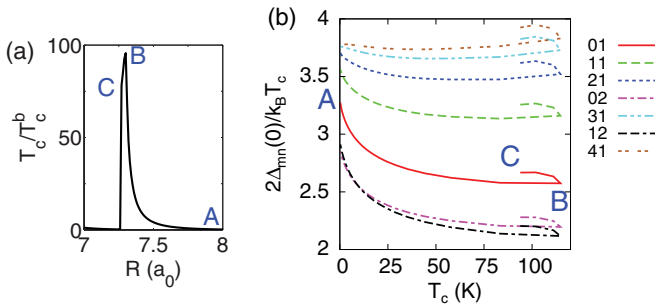


FIG. 3. (Color online) (a) T_c for a range of small radii R , in which it varies very strongly, starting with a value of 0.29 K ($0.24T_c^b$) at A, reaching a maximum value of 115 K ($96T_c^b$) at B, and decreasing to 94 K ($78T_c^b$) at C. (b) Plot of the ratios $2\Delta(T)/k_B T_c$ vs T_c . In spite of the very high- T_c values attained, the ratios fall in the range of values for conventional superconductors in the Inosov plot [cf. Ref. 22]. The range of T_c values considered corresponds to the radii in plot (a).

in line with the expectation that the Inosov plot discriminates between conventional and unconventional superconductors. On the other hand, the nanowire results seem to insist on the idea that a high- T_c value may not necessarily require a particularly strong or unconventional pairing interaction, and that a suitable electronic structure (e.g., Fermi surface topology, density of states behavior) might be as important as the energy scale of the pairing mechanism.

Another property that is widely used to characterize superconductors is the superfluid density. Its temperature dependence, for instance, is used to try to determine the symmetry of the order parameter, or to find signs of unconventional superconductivity.³⁹ We can calculate the superfluid density at temperature T in a nanowire through

$$n_s(T) = \frac{1}{\pi R^2 L} \int d^3 r d^3 r' |\Psi(\mathbf{r}\mathbf{r}')|^2, \quad (17)$$

with $\Psi(\mathbf{r}\mathbf{r}')$ given by Eq. (10). One readily finds $n_s(T) = \sum_{m \geq 0, n} (2 - \delta_{m0})^2 C_{mn} / 16\pi^2 R^2$, with

$$C_{mn} = \int_{-\epsilon_w}^{+\epsilon_w} d\epsilon \frac{\tanh^2 \frac{\sqrt{\epsilon^2 + \Delta_{mn}^2}}{2k_B T}}{(\epsilon^2 + \Delta_{mn}^2) \sqrt{\epsilon^2 - \hbar^2 \eta_{mn}^2 / 2mR^2 + \mu}}. \quad (18)$$

The superfluid density is typically very low compared to the total electron density. For example, for $R = 7.5 a_0$ we have $n_s/n = 3.45 \times 10^{-5}$. This follows from the fact that the states that form Cooper pairs are only those in an energy window around the Fermi level that is very small compared to the total bandwidth.⁴⁰ In Fig. 4 we show our result for $n_s(T)/n_s(0)$. We can see that confinement results in a clear deviation from the empirical behavior of conventional, phonon mediated, bulk superconductors, the latter following a $1 - (T/T_c)^4$ behavior.²⁰ Among approximations of the form $1 - (T/T_c)^n$, the closest to our result is for $n = 3$. Thus, our curve also deviates from the behavior predicted BCS theory for homogeneous systems. Indeed, in the local limit that later results in $n_s(T)/n = 2(1 - T/T_c)$ close to T_c , while in the nonlocal limit (not shown in Fig. 4) it results in a curve close

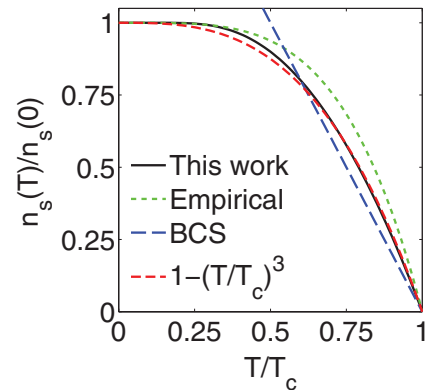


FIG. 4. (Color online) Plot of the temperature dependence of the (normalized) superfluid density, showing that near T_c it deviates from both the BCS local [$2(1 - T/T_c)$] and nonlocal behaviors. The latter is close to the empirical behavior of conventional superconductors [$1 - (T/T_c)^4$].²⁰ The best fit to our result near T_c is of the form $1 - (T/T_c)^3$.

to the empirical form.²⁰ The result for other nanowire radii is similar.

IV. DISCUSSION

To conclude, some comments are in order regarding some of the assumptions or approximations made in deriving our results. Nanowires are strongly anisotropic systems. Hence the effective mass is likely to be anisotropic as well. Taking this into account will change the density of states, resulting in, for example, a change in the T_c dependence on nanowire radius. The qualitative behavior, however, will remain the same. Another important approximation, with strong quantitative consequence, is that the strength of the contact interaction was taken equal to its bulk value. This assumes that the phononic and dielectric properties of the nanowire are the same as those of the bulk. This is a difficult point, but to make progress toward a quantitative theory in the future it will be important to address it. Indeed, we applied the present calculation scheme to nanofilms, taking into account the effects of confinement on the screened electron-ionic background interaction. We found that the latter is weakened when the electronic density of states increases, leading to a decrease

of electron-phonon coupling.⁴¹ This possible effect in bulk superconductors was already pointed out in Ref. 37. This has an important bearing on the role of shape resonances in the observed dependence of T_c on nanowire radius. As we saw above, in the present scheme, when the Fermi level is close to a van Hove singularity, the values of the critical parameters, such as T_c and gap values, can be very large. But it is not clear that this will still be the case with a more accurate description of electron-phonon coupling. It is also probably very difficult experimentally to tune the radius of a nanowire so finely. Maybe some steps in this direction can be taken by doping. One must recall, nevertheless, that in the electron gas a peak in the density of states leads to a peak in the specific heat. This signals an instability that may be resolved by a phase transition, either structural or electronic (e.g., transition to a ferromagnetic phase), taking place already in the normal state. So it may be intrinsically difficult to exploit the van Hove singularities to obtain very high critical parameters.

ACKNOWLEDGMENTS

This work was supported by FWO-VI and the Belgian Science Policy (IAP).

¹O. S. Lutes, *Phys. Rev.* **105**, 1451 (1957).

²J. M. Blatt and C. J. Thompson, *Phys. Rev. Lett.* **10**, 332 (1963).

³C. J. Thompson and J. M. Blatt, *Phys. Lett.* **5**, 6 (1963).

⁴C. G. Granqvist and T. Claeson, *Phys. Rev. Lett.* **31**, 456 (1973).

⁵G. Yi and W. Schwarzacher, *Appl. Phys. Lett.* **74**, 1746 (1999).

⁶D. Y. Vodolazov, F. M. Peeters, L. Piraux, S. Mátéfi-Tempfli, and S. Michotte, *Phys. Rev. Lett.* **91**, 157001 (2003).

⁷M. Tian, J. Wang, J. S. Kurtz, Y. Liu, M. H. W. Chan, T. S. Mayer, and T. E. Mallouk, *Phys. Rev. B* **71**, 104521 (2005).

⁸Y. S. Hor, U. Welp, Y. Ito, Z. L. Xiao, U. Patel, J. F. Mitchell, W. K. Kwok, and G. W. Crabtree, *Appl. Phys. Lett.* **87**, 142506 (2005).

⁹M. Tian, J. Wang, N. Kumar, T. Han, Y. Kobayashi, Y. Liu, T. E. Mallouk, and M. H. W. Chan, *Nano Lett.* **6**, 2773 (2006).

¹⁰M. Zgirski and K. Y. Arutyunov, *Phys. Rev. B* **75**, 172509 (2007).

¹¹L. Jankovič, D. Gournis, P. N. Trikalitis, I. Arfaoui, T. Cren, P. Rudolf, M.-H. Sage, T. T. M. Palstra, B. Kooi, J. De Hosson, M. A. Karakassides, K. Dimos, A. Moukarika, and T. Bakas, *Nano Lett.* **6**, 1131 (2006).

¹²N. Tombros, L. Buit, I. Arfaoui, T. Tsoufis, D. Gournis, P. N. Trikalitis, S. J. van der Molen, P. Rudolf, and B. J. van Wees, *Nano Lett.* **8**, 3060 (2008).

¹³A. A. Shanenko, M. D. Croitoru, M. Zgirski, F. M. Peeters, and K. Y. Arutyunov, *Phys. Rev. B* **74**, 052502 (2006).

¹⁴In this connection it is interesting to mention that it has been observed that the critical temperature in Al grains can be significantly enhanced, depending on grain size. For a recent review, see G. Deutscher, in *Superconductivity*, edited by K. H. Bennemann and J. B. Ketterson, Vol. I (Springer, Berlin, 2008), p. 259.

¹⁵F. M. Peeters, A. A. Shanenko, and M. D. Croitoru, in *Handbook of Nanophysics*, edited by Klaus D. Sattler (Taylor & Francis, London, 2010).

¹⁶P. G. de Gennes, *Superconductivity of Metals and Alloys* (W. A. Benjamin, New York, 1966).

¹⁷J. E. Han and V. H. Crespi, *Phys. Rev. B* **69**, 214526 (2004).

¹⁸A. A. Shanenko and M. D. Croitoru, *Phys. Rev. B* **73**, 012510 (2006).

¹⁹A. A. Shanenko, M. D. Croitoru, A. Vagov, and F. M. Peeters, *Phys. Rev. B* **82**, 104524 (2010).

²⁰A. L. Fetter and J. D. Walecka, *Quantum Theory of Many-Particle Systems* (McGraw-Hill, New York, 1971).

²¹L. P. Gor'kov, *Sov. Phys. JETP* **7**, 505 (1958).

²²D. S. Inosov, J. T. Park, A. Charnukha, Yuan Li, A. V. Boris, B. Keimer, and V. Hinkov, *Phys. Rev. B* **83**, 214520 (2011).

²³Chr. Bruder, *Phys. Rev. B* **41**, 4017 (1990).

²⁴A. Pastore, F. Barranco, R. A. Broglia, and E. Vigezzi, *Phys. Rev. C* **78**, 024315 (2008).

²⁵The sign introduced is for notational convenience; our final expressions for the Green function and gap equation have thus the same signs as in textbook expressions, such as Ref. 20.

²⁶P. W. Anderson, *J. Phys. Chem. Solids* **11**, 26 (1959).

²⁷A. J. Leggett, in *Superconductivity*, edited by K. H. Bennemann and J. B. Ketterson, Vol. II (Springer, Berlin, 2008), p. 1517.

²⁸The particle density is $r_s = 2.07 a_0$ and the bulk critical temperature $T_c^b = 1.2$ K; for reference further down, the bulk density of states per spin (N_0) is obtained with the electron gas expression,²⁹ and $\hbar\omega_D/k_B = 375$ K.²⁰

²⁹N. W. Ashcroft and N. D. Mermin, *Solid State Physics* (Saunders College, Philadelphia, 1976).

³⁰M. Abramowitz and I. Stegun, eds., *Handbook of Mathematical Functions* (Dover, New York, 1972).

³¹For V_0 we use the BCS coupling constant for the bulk material, estimated from the experimental value of T_c and $k_B T_c = 1.13\hbar\omega_D e^{-1/N_0 V_0}$.²⁰ It is not obvious that this value is appropriate for a nanowire, but it was shown to be reasonable for a qualitative discussion.^{17,18} One has

$$U_{mn,m'n'} = 2V_0 \int_0^1 dx x \frac{J_m^2(x\eta_{mn})}{J_{m+1}^2(\eta_{mn})} \frac{J_{m'}^2(x\eta_{m'n'})}{J_{m'+1}^2(\eta_{m'n'})}.$$

- ³²If a band minimum $E_{0mn} = \hbar^2 \eta_{mn}^2 / 2mR^2$ happens to fall within the energy window $\mu \pm \epsilon_w$, then the lower limit of the integral in Eq. (13) is given instead by $\mu - E_{0mn}$.
- ³³K. Tanaka and F. Marsiglio, *Phys. Rev. B* **62**, 5345 (2000).
- ³⁴N. Kristoffel, T. Örd, and K. Rágo, *Europhys. Lett.* **61**, 109 (2003).
- ³⁵F. Giubileo, D. Roditchev, W. Sacks, R. Lamy, D. X. Thanh, J. Klein, S. Miraglia, D. Fruchart, J. Marcus, and Ph. Monod, *Phys. Rev. Lett.* **87**, 177008 (2001).
- ³⁶O. V. Dolgov, I. I. Mazin, D. Parker, and A. A. Golubov, *Phys. Rev. B* **79**, 060502 (2009).
- ³⁷G. D. Mahan, *Phys. Rev. B* **48**, 16557 (1993).
- ³⁸For radii below that of point C, the ratios show a pattern similar to the one just described.
- ³⁹H. Luetkens, H.-H. Klauss, R. Khasanov, A. Amato, R. Klingeler, I. Hellmann, N. Leps, A. Kondrat, C. Hess, A. Köhler, G. Behr, J. Werner, and B. Büchner, *Phys. Rev. Lett.* **101**, 097009 (2008).
- ⁴⁰In experiment the superfluid density is usually studied through the magnetic penetration depth. For reference we note that using the London expression ²⁰ $\lambda^2 = mc^2 / 4\pi n_s e^2$ yields $\lambda \simeq 21272$ Å for our example with $R = 7.5 a_0$. This is much longer than the penetration depth in bulk Al (~ 500 Å).^{16,20} We caution, however, that it is not clear at all that the London expression applies. A more specific calculation for nanosystems is probably required.
- ⁴¹R. Saniz, B. Partoens, and F. M. Peeters (to be published).